PHYSICAL REVIEW D **95,** 025008 (2017)

Standard model vacuum decay with gravity

Arttu Rajantie and Stephen Stopyra
Department of Physics, Imperial College London, London SW7 2AZ, United Kingdom
(Received 10 June 2016; published 10 January 2017)

We present a calculation of the decay rate of the electroweak vacuum, fully including all gravitational effects and a possible nonminimal Higgs-curvature coupling ξ, and using the three-loop Standard Model effective potential. Without a nonminimal coupling, we find that the effect of the gravitational backreaction is small and less significant than previous calculations suggested. The gravitational effects are smallest, and almost completely suppressed, near the conformal value $\xi = 1/6$ of the nonminimal coupling. Moving ξ away from this value in either direction universally suppresses the decay rate.

DOI: 10.1103/PhysRevD.95.025008

I. INTRODUCTION

Since the discovery of the Higgs boson in 2012 [1,2], there has been considerable interest in the phenomenon of vacuum decay, motivated by calculations which suggest that the Standard Model effective potential is unstable for the observed value of the Higgs boson and top quark masses [3–5]. The observed masses place the Standard Model firmly in the metastability zone, i.e., there exists a second minimum of the potential at much larger field values, to which the electroweak vacuum can decay via the nucleation of bubbles of true vacuum, with the expected lifetime of the visible Universe being longer than its age by many orders of magnitude [6]. The nonoccurrence of such a bubble nucleation event is not inconsistent with this long lifetime; however, the possibility of vacuum decay places constraints on high-energy phenomena which might result in the nucleation of true vacuum bubbles. The implications for inflation with a high Hubble rate, for example, have been investigated by many authors [7–11].

Lately, there has also been renewed interest in the effect of gravitational backreaction on vacuum decay in the Standard Model. Calculations show that vacuum decay is dominated by the formation of bubbles with a scale only a single order of magnitude below the Planck scale [12], where the effect of gravity might be expected to start appearing. The Standard Model effective potential in this regime is negative, and thus the space-time at the center of such a bubble is locally anti–de Sitter (AdS), albeit with a sub-Planckian energy density. It was shown by Coleman and de Luccia [13], using the thin-wall approximation, that a transition from a zero-energy-density, false vacuum to a negative-energy-density, true vacuum leads to a suppression of the decay rate, due to the warped geometry of the nucleated bubbles. An early paper by Isidori *et al.* [14] used a perturbative series in the gravitational coupling to try and estimate the size of this effect. However, it was pointed out recently by Branchina *et al.* [15] that the boundary conditions of the perturbative bounce solution are not satisfied to first order (see discussion section). Additionally, Gregory and Moss *et al.*, in three recent papers [16–18], investigated vacuum decay in a black-hole background, finding that a black hole can effectively "seed" vacuum decay, in analogy with phase transitions in condensed matter systems.

Recent papers have investigated gravitational effects using quartic model potentials; these have the advantage of being easy to compare to the thin-wall results. Branchina *et al.* [15] found that the suppression effect was much less significant, when compared to the thin-wall approximation, for properly treated thick-wall bubbles. Masoumi, Paban, and Weinberg also investigated the thin-wall approximation [19]; they showed that energy arguments for when bubbles may form in the presence of gravitational backreaction can be extended to thick-wall bubbles and also demonstrated that the tunneling rate is not affected by the presence of a Gibbons-Hawking-York boundary term in the action.

Another factor, when gravity is included, is the possible presence of a nonminimal coupling between the Higgs field and space-time curvature. It cannot be consistently omitted because—even if it is zero or near zero at present scales—it will run and become nonzero at higher energies. Therefore it is required for the renormalizability of a scalar field in curved space-time [20]. Previously this has been investigated in an inflationary background [10]. So far, however, these results have not been extrapolated to the case of a flat-space false vacuum. Fortunately, the effect of nonminimal coupling with only a small cosmological constant, as in the present day, can be approximated by treating the false vacuum as flat space-time. In this paper we calculate bounce solutions for the Standard Model effective potential, with a nonminimal coupling term $\xi\phi^2 R/2$ included in the action. We compute the solutions for the three-loop Standard Model effective potential by making use of the three-loop beta functions (with two-loop pole-matching) available in the literature [21,22], with which we construct an interpolated potential that can be computed quickly at each step in a numerical integration. We find that the effect of backreaction on the boundary between instability and

metastability is small. Furthermore, for a flat-space false vacuum, nonminimal coupling always suppresses Standard Model vacuum decay relative to the flat-space calculation without backreaction, regardless of the sign of ξ. We also find that the conformal value of the coupling, i.e., $\xi = 1/6$ rather than $\xi = 0$, leads to near cancellation of the backreaction, producing a bounce nearly identical to the flat-space bounce. The conformal coupling is found to be a (near) minimum of the decay exponent when ξ is varied, and an exact minimum for the $\lambda\phi^4/4$ potential. We show that if the running of the Higgs coupling did not break the conformal symmetry of the $\lambda\phi^4/4$ potential then this near cancellation would be exact and the resulting bounces would be identical to flat space. Finally, we present a comparison of our results with the perturbative method of Ref. [14].

II. BOUNCES WITH NONMINIMAL COUPLING

The decay rate of a metastable vacuum state is given, in the semiclassical approximation, by the Coleman formula [23]:

$$\Gamma = Ae^{-B}, \tag{1}$$

where $B = S - S_0$ is the difference in Euclidean action between two solutions of the Euclidean field equations of the theory. S is the action of a so-called bounce solution which interpolates between the false and true vacua (though it does not in general reach the true vacuum), while S_0 is the action of a constant solution sitting at the false vacuum. The prefactor A is determined, at the semiclassical level, by a functional determinant and is known in the flat-space case (see Ref. [12]), but has yet to be computed in a curved background. The Euclidean action for a scalar (Higgs) field nonminimally coupled to gravity is

$$S = \int \mathrm{d}^4x\sqrt{|g|}\left[\frac{1}{2}\nabla^\mu\phi\nabla_\mu\phi + V(\phi) + \frac{1}{2}\xi\phi^2 R - \frac{M_\mathrm{P}^2}{2}R\right], \tag{2}$$

where $M_\mathrm{P} = 1/\sqrt{8\pi G_N}$ is the reduced Planck mass. This modifies the original action considered by Coleman and de Luccia [13] to include a possible nonminimal coupling between the scalar field and gravity. This is required to be present for the theory to be renormalizable [10,20]. A cosmological constant can also be included, but here it has been absorbed into the definition of the potential $V(\phi)$. We neglect boundary terms, which can be dealt with by adding a Gibbons-Hawking-York term to the action [24], and they do not contribute to the decay rate because the two solutions are identical on the boundary of the Euclidean space-time, if it has a boundary: see Ref. [19] for a recent discussion of these boundary terms.

One way to deal with this system is to perform a nonlinear field transformation $(\phi, g_{\mu\nu}) \to (\tilde{\phi}, \tilde{g}_{\mu\nu})$, to the Einstein frame (see the Appendix for details), in which the action takes the form

$$S = \int \mathrm{d}^4x\sqrt{|\tilde{g}|}\left[\frac{1}{2}\tilde{g}^{\mu\nu}\nabla_\mu\tilde{\phi}\nabla_\nu\tilde{\phi} + \frac{V(\phi(\tilde{\phi}))}{\left(1-\frac{\xi\phi(\tilde{\phi})^2}{M_\mathrm{P}^2}\right)^2} - \frac{M_\mathrm{P}^2}{2}\tilde{R}\right]. \tag{3}$$

It should be emphasized that this transformation does not change the action, since by definition it is a transformation of the fields alone: Eq. (3) is obtained by a transformation of the field variables in Eq. (2), which does not affect the value of the integral. Since, at the semiclassical level, the action is the quantity of interest for computing a decay rate, the frame in which the action is computed does not matter. The Einstein frame makes clearer the link between bounce solutions with a nonminimal coupling term, and the original formulation of Coleman–de Luccia bounces which are defined in terms of an action resembling Eq. (3) [13]. In particular, if a bounce is $O(4)$ symmetric in the Einstein frame, then it will be $O(4)$ symmetric in the Jordan frame [as the transformations (A1) and (A4) do not transform an $O(4)$-symmetric solution into a non-$O(4)$-symmetric solution]. It is assumed here that bounces are $O(4)$ symmetric in the Einstein frame. This is strictly speaking only a conjecture for Coleman–de Luccia bounces: it has been proven in flat space [25], but we know of no proof in the curved-space case. Several studies, however, have indicated that it is likely to hold [26,27].

For computational purposes, however, the Einstein frame is inconvenient. The principle reason for this is that evaluation of the Einstein-frame potential

$$\tilde{V}(\phi(\tilde{\phi})) = \frac{V(\phi(\tilde{\phi}))}{\left(1-\xi\phi(\tilde{\phi})^2/M_\mathrm{P}^2\right)^2}, \tag{4}$$

requires evaluating $\phi(\tilde{\phi})$, the inverse of Eq. (A4). This inverse is not known in closed form, so each call to the potential requires inverting Eq. (A4) numerically. Consequently, it is more convenient to perform the calculation in the Jordan frame. The resulting (Jordan-frame) Euclidean field equations are

$$R_{\mu\nu} - \frac{1}{2}g_{\mu\nu}R = \frac{T_{\mu\nu} + \xi[-\nabla_\mu\nabla_\nu\phi^2 + g_{\mu\nu}\nabla_\lambda\nabla^\lambda\phi^2]}{M_\mathrm{P}^2\left(1-\xi\frac{\phi^2}{M_\mathrm{P}^2}\right)}, \tag{5}$$

$$T_{\mu\nu} \equiv \nabla_\mu\phi\nabla_\nu\phi - g_{\mu\nu}\left[\frac{1}{2}\nabla_\lambda\phi\nabla^\lambda\phi + V(\phi)\right],$$
$$\nabla_\mu\nabla^\mu\phi = V'(\phi) + \xi\phi R. \tag{6}$$

Note that Einstein's field equations acquire an additional term on the RHS, arising from the $\delta R_{\mu\nu}$ term in the variation of the action which does not immediately form a total derivative term (as is the case in the variation of the usual Einstein-Hilbert action) due to the position-dependent prefactor $1-\xi\phi^2/M_{\rm P}^2$. Under the assumption of $O(4)$ symmetry, there is a coordinate system in which the metric takes the form

$$ds^2 = d\chi^2 + a^2(\chi)d\Omega_3^2, \tag{7}$$

where $d\Omega_3^2$ is the unit metric on a 3-sphere. The coordinate χ is the radial distance from the origin, while $a(\chi)$ is the radius of curvature of a 3-sphere at fixed radius χ. Using this coordinate system, the equations of motion take the form

$$\ddot{\phi} = -\frac{3\dot{a}}{a}\dot{\phi} + V'(\phi) + \xi\phi R, \tag{8}$$

$$\dot{a}^2 - 1 = -\frac{a^2[-\frac{\dot{\phi}^2}{2} + V(\phi) - \frac{6\xi\dot{a}\phi\dot{\phi}}{a}]}{3M_{\rm P}^2(1-\frac{\xi\phi^2}{M_{\rm P}^2})}, \tag{9}$$

$$\ddot{a} = -\frac{a[\dot{\phi}^2 + V(\phi) - 3\xi(\dot{\phi}^2 + \phi\ddot{\phi} + \frac{\dot{a}}{a}\phi\dot{\phi})]}{3M_{\rm P}^2(1-\frac{\xi\phi^2}{M_{\rm P}^2})}, \tag{10}$$

$$R = \frac{\dot{\phi}^2(1-6\xi) + 4V(\phi) - 6\xi\phi V'(\phi)}{M_{\rm P}^2[1-\frac{\xi(1-6\xi)\phi^2}{M_{\rm P}^2}]}, \tag{11}$$

where dots indicate differentiation with respect to χ. Equation (10) is equivalent to the derivative of Eq. (9); however, we include it here as it is more reliable for numerics (see Sec. III). The boundary conditions for the bounce are imposed so that the action difference is finite, and they depend on the asymptotic behavior of $a(\chi)$:

(1) If there exists $\chi_{\rm max} > 0$ such that $a(\chi_{\rm max}) = 0$, the Euclidean space-time is compact; we impose $\dot{\phi}(0) = \dot{\phi}(\chi_{\rm max}) = 0$ to prevent ϕ from diverging due to the $1/a$ coordinate singularity when $a \to 0$.
(2) If $a(\chi)$ does not cross zero as $\chi \to \infty$, the Euclidean space-time is noncompact and $\phi(\chi) \to \phi_{\rm fv}$ at infinity (where $\phi_{\rm fv}$ is the field in the false vacuum) in order that $S - S_0$ remains finite.

The boundary condition $a(0) = 0$, required to solve Eq. (9), is imposed in both cases. The two scenarios are qualitatively different; the compact space-time of the first gives rise to an effective temperature, and corresponds to a combination of thermal excitation and tunneling in a de Sitter-like space-time (see Ref. [28] for a discussion). In this paper we focus on the second case, which is the behavior in the Standard Model if the false vacuum is exactly flat space-time.

Additionally, note the singularity appearing in the Einstein-frame potential for $\xi > 0$ at $\phi = M_{\rm P}/\sqrt{\xi}$. This is not simply an artifact of the conformal transformation, as it is also present in Eq. (10). Finite action bounce solutions cannot touch higher field values than this. Since bounces in the Standard Model neglecting gravity are controlled by a scale an order of magnitude below the Planck scale [12], it is reasonable to conclude that (a) gravitational backreaction of the bounce may have an impact, and (b) nonminimal coupling will necessarily distort the peak of the bounce solution. As is clear from Eq. (4), the effect of nonminimal coupling is negligible if $\phi \ll M_{\rm P}/\sqrt{|\xi|}$, but it is strong above this.

III. NUMERICAL METHODS

An important numerical challenge for bounce calculations including gravitational effects is that the bounce solutions in a dS-like background do not necessarily touch the false vacuum [28,29]; this is a property allowed by the compact nature of the Euclidean analogue of dS-like spaces. As a result, large (and in the flat-space limit, infinite) contributions to the decay exponent $B = S[\phi_{\rm bounce}] - S[\phi_{\rm fv}]$ do not cancel explicitly between the bounce and false-vacuum actions (as is the case in the fixed background approximation). Instead a "near cancellation" must occur numerically, which is difficult to study without very high-precision calculations. Fortunately, transitions from flat false vacua to AdS true vacua do not suffer from this problem as the Euclidean analogues are noncompact and the bounce solution must touch the false vacuum. It makes sense, therefore, to ignore the small observed positive cosmological constant and consider transitions from a flat false vacuum to an AdS-like true vacuum. In this paper, we focus on the case of a flat false vacuum. Physically, it is plausible that the decay rate does not depend on the small cosmological constant, since the length scale of the bounces we find is many orders of magnitude smaller than the length scale associated to the small observed cosmological constant. [One can make this more quantitative by comparing the bounce energy density, $E = \frac{\dot{\phi}^2}{2} - V(\phi)$ to the cosmological constant energy density V_0; for our bounces we find $V_0/|E| \ll 1$ everywhere, indicating that solution is virtually unchanged.] The precise nature of the $V_0 \to 0$ limit, however, will be investigated in a future paper.

We use an overshoot/undershoot method to find the bounce solution, as originally proposed in Ref. [13]. Note that we solve Eq. (10) rather than Eq. (9) for the numerics in this paper in order to avoid the square root ambiguity when $\dot{a}$ passes through zero, which happens in a de Sitter background [for example, in a fixed de Sitter background with Hubble rate H the solution is $a(\chi) = \sin(H\chi)/H$]. We treat Eq. (9) as a constraint which imposes the second boundary condition [$\dot{a}(0) = +1$] required by Eq. (10). This

does not affect the results for transitions from flat false vacua to AdS true vacua since $\dot{a} > 0$ everywhere for such cases, but it is more generally applicable.

To solve the ordinary differential equations (ODEs) (8) and (10), we made use of the Odeint library for C++ [30]. This library was chosen because it is highly modular in its design and can support a range of different variable types; in particular it naturally supports several types of variable precision numbers. We used the MPFR implementation of the GNU multiprecision library [31,32] as the variable-precision back end. The code uses variable-precision numbers for two reasons: (a) so that it can resolve the vast range of scales (electroweak, barrier scale, λ minimization scale, and Planck scale) present in the Standard Model with sufficient precision, and (b) so that it can also be used to study backreaction in a de Sitter background. In de Sitter there is an additional numerical challenge because the boundary conditions do not require ϕ to touch the false vacuum; when backreaction is taken into account, S_0 does not cancel analytically in $S - S_0$, as in the fixed background approximation, and since $|S_0| \sim O(M_P^4/V) \gg |S - S_0|$ generically, rounding errors will wash out the backreaction if not under stringent control.

To approximate the Standard Model potential, we use a piecewise polynomial to interpolate the running of the self-coupling, $\lambda(t(\mu))$ where $t = \ln(\mu^2/M^2)$. Choosing $\mu = \phi$, the Higgs potential at large scales can be approximated as

$$V_{\mathrm{SM}}(\phi) = \frac{\lambda(t(\phi))\phi^4}{4}. \tag{12}$$

We form an approximation of this potential starting from $N+1$ discrete points $\lambda_i = \lambda(t_i)$, $i = 0, 1, 2, \ldots, N$ obtained by solving the beta functions, which are available in the literature [6,21,22], and then fitting N cubic polynomials $\lambda_n(t), n = 1, 2, \ldots, N$, each defined only between t_{n-1} and t_n:

$$\lambda_n(t) = [1 - x_n(t)]\lambda_{n-1} + x_n(t)\lambda_n + x_n(t)[1 - x_n(t)]\{a_n[1 - x_n(t)] + b_n x_n(t)\}, \tag{13}$$

$$x_n(t) \equiv \frac{t - t_{n-1}}{t_n - t_{n-1}}, \tag{14}$$

$$a_n = k_{n-1}(t_n - t_{n-1}) - (\lambda_n - \lambda_{n-1}), \tag{15}$$

$$b_n = -k_n(t_n - t_{n-1}) + (\lambda_n - \lambda_{n-1}). \tag{16}$$

The constants k_n are the derivatives [with respect to $t = \ln(\phi^2/M^2)$] of the polynomial, at t_n. These are chosen to equal the derivatives of λ, $\mathrm{d}\lambda/\mathrm{d}t = \beta_\lambda(t)$, resulting in a C_1 continuous piecewise approximation of $\lambda(t)$. An alternative choice is to pick k_n such that the piecewise polynomial is C_2 continuous; such an approximation is known as a cubic spline [33]. However, we found that this led to unwanted oscillation effects in the potential. Figure 1 shows an example interpolated potential compared to the exact values predicted by solving the beta functions. Using this approximation, it is possible to create a model of the Standard Model potential which is arbitrarily close to the true Standard Model potential simply by taking more initial points to interpolate between. Note that for nonlinearly spaced points t_i (e.g., the output of an adaptive ODE solver), selecting the correct polynomial for an arbitrary input ϕ may require an interpolative search: since such a search requires on average $O(\log(\log(N)))$ steps [34], this is not generally a problematic bottleneck.

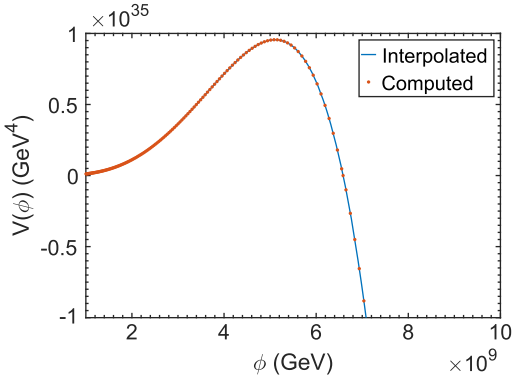

FIG. 1. Interpolated potential for $M_t = 173.34$ GeV, $M_h = 125.15$ GeV, compared to "exact" values obtained by solving the beta functions numerically.

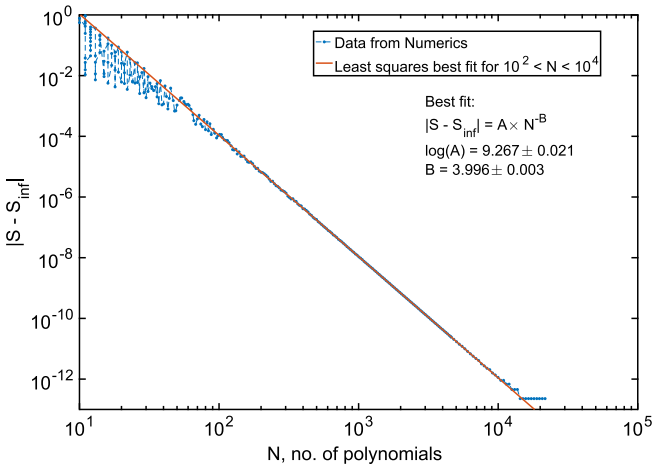

FIG. 2. Difference between the action as a function of N and the action at large N (used as a proxy for $N \to \infty$). For small N, the behavior deviates from power-law behavior as the shape of the potential settles down. Beyond this, the sampling intervals are smaller than the variations in the potential, and the action settles down, approaching the large-N action with a difference decreasing as a negative power of N. The apparent deviation at large N is due to the floating-point double-precision limit for the action (around 10^{-13} for $S \sim 10^3$, as is the case here), which is stored at double precision for data processing, and is not a real effect.

To check how reliable this interpolated potential is, we can compute the action for different numbers of interpolating functions, N. Figure 2 shows the difference between the action as a function of N and the action for the highest N considered, $S_{\rm inf}$, which is used as a proxy for the unknown action as $N \to \infty$. This demonstrates that the evolution of $S - S_{\rm inf}$ with N is very well approximated by power-law convergence. In this paper, we use $N \sim O(10^4)$ (the precise number is chosen by an adaptive integration routine for the beta functions, and thus varies).

IV. RESULTS

Figure 3 illustrates a few example bounce solutions for different values of ξ, compared with the flat-space equivalent. Most notable is $\xi = 1/6$, which is almost (but as the inset plot shows, not quite) identical to the flat-space case. The boundary value $\phi(0)$ for each bounce is constrained by the overshoot/undershoot method to a range of width $\sim 10^{-15}$, much smaller than the difference between the initial values for $\xi = 0$ and $\xi = 1/6$, while the solutions are computed with an absolute error tolerance of 10^{-20} using arbitrary precision variables. This verifies that the small difference between the $\xi = 1/6$ and $\xi = 0$ solutions is not simply a numerical artifact. The effects of positive and negative ξ on the bounce are qualitatively similar.

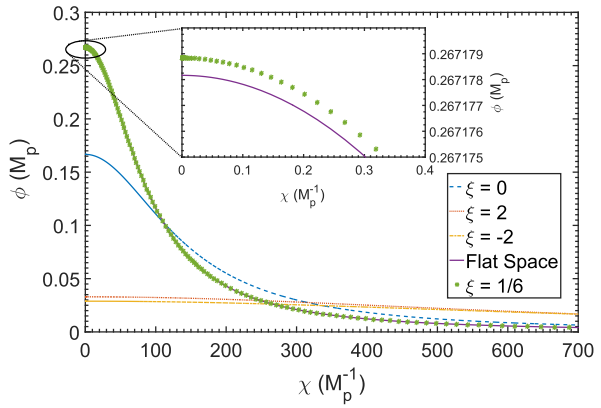

FIG. 3. Bounce solutions as a function of distance χ from the center of the bounce, computed for various values of ξ. The $\xi = 1/6$ solution is extremely close to the flat-space solution (though not identical to it). A larger $|\xi|$ tends to flatten and broaden the bounce, as does the inclusion of backreaction for $\xi = 0$.

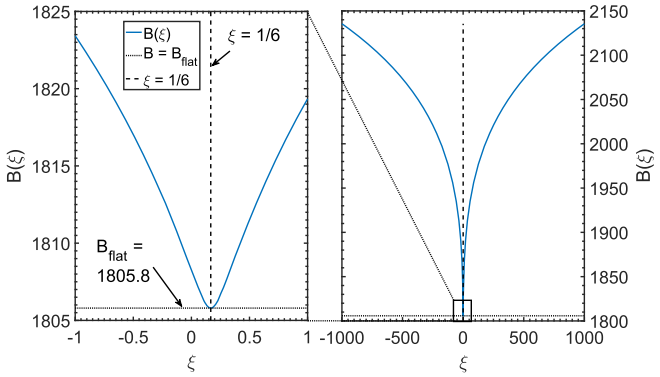

FIG. 4. Decay exponent for different values of ξ at $M_t = 173.34$ GeV, $M_h = 125.15$ GeV, compared with the flat-space result. Left: Variation around the minimum near $\xi = 1/6$. Right: Large-scale variation of $B(\xi)$.

Figure 4 shows how this affects the decay rate. As with the bounce, the $\xi = 1/6$ case is virtually identical to the flat-space case, and represents the approximate minimum decay exponent. For both positive and negative values of ξ away from $\xi = 1/6$, the decay rate is suppressed, increasingly so as ξ is increased. This trend continues to much larger values of ξ, until around $\xi \sim 10^{18}$, where the barrier is erased in Eq. (4). Figure 5 shows the same curve as Fig. 4 but around the minimum, demonstrating the slight deflection from $\xi = 1/6$ and that the curve always lies above the flat-space case. To verify that this is not a numerical artifact, this figure is generated using 56 642 interpolating polynomials for the running of λ, with the bounce equations solved at an absolute tolerance of 10^{-20} using arbitrary precision variables.

We also computed the effect of varying ξ on the boundary between metastability and instability. Lacking a complete analysis of the A coefficient in Eq. (1), which requires a computation of the functional determinant including graviton loops, we estimate the lifetime by assuming $A \sim 1/\bar{R}^4$ where $\bar{R}$ is the full-width-half-maximum of the bounce (this is a good approximation of the quantum corrections in the flat-space case [12,35]). This results in a lifetime of [35]

$$\frac{\tau}{T_U} = \left(\frac{\bar{R}}{T_U}\right)^4 e^B, \tag{17}$$

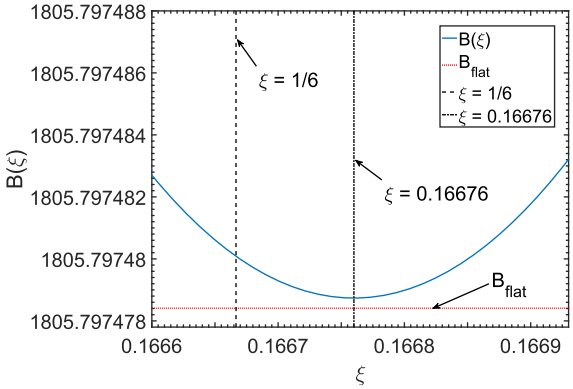

FIG. 5. High-resolution data around the minimum of $B(\xi)$ for $M_t = 173.34$ GeV, $M_h = 125.15$ GeV. This demonstrates that the true minimum is slightly deflected from $\xi = 1/6$ and that the decay, even at the minimum, is suppressed relative to the flat-space case.

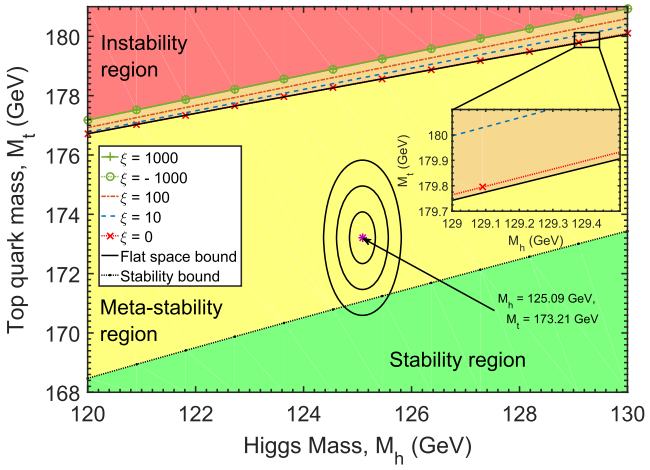

FIG. 6. Instability/metastability boundaries computed for different values of ξ. With $\xi = 0$, the bounds hardly shift at all from the flat-space bound (see the inset which shows that the nearly coincident flat-space and $\xi = 0$ with backreaction boundaries are in fact separate, albeit very close). With increasing $|\xi|$, the instability region is pushed back; notice that this is true for both positive and negative ξ—the boundaries for $\xi = \pm 1000$ are nearly coincident. The Standard Model parameter uncertainty region around $M_h = 125.09$ GeV, $M_t = 173.21$ GeV [36] with 1, 2, and 3 sigma bounds is shown for reference.

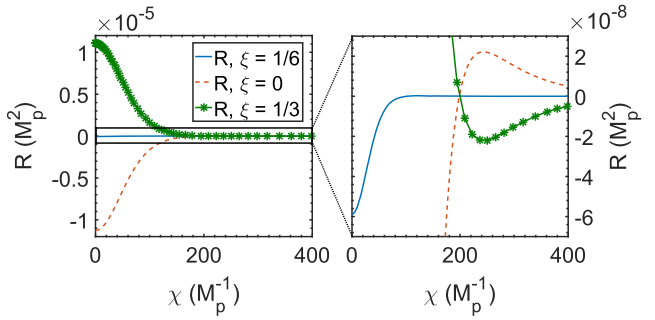

FIG. 7. Ricci scalar with distance from the center of the bounce, in the $\xi = 0$, $\xi = 1/6$ and $\xi = 1/3$ cases with $M_t = 173.34$ GeV, $M_h = 125.15$ GeV. For $\xi = 1/3$, R is positive in the interior of the bounce.

where T_U is the age of the visible Universe. Although a full analysis of the functional determinant in the flat-space case is available [12], we use Eq. (17) as an estimate in the flat-space case in order to separate out the effect of backreaction alone. As a consequence, our bounds on the metastability/instability regions sacrifice accuracy in order to demonstrate the effect of backreaction. The resulting change in the instability/metastability boundary, which we define as the curve where $\tau = T_U$, is plotted in Fig. 6.

V. DISCUSSION

A. Backreaction

Figure 6 appears to suggest that the effect of gravitational backreaction on vacuum decay is almost negligible when $\xi = 0$. Even near the instability boundary, the lifetime of the vacuum would not shift significantly due to gravitational effects, despite the change in the shape of the bounce. This appears to support the findings of the authors of Ref. [15], who studied the effect of backreaction on vacuum instability in a quartic model potential. They found that the thin-wall approximation overestimated the effect of backreaction in suppressing vacuum decay compared to the true thick-wall bubbles and argued that the inclusion of gravitational backreaction would not stabilize the potential against decay, even in a strong gravity regime. The bounces we calculated for the actual Standard Model potential are thick-wall bubbles and appear to bear this out; the gravitational backreaction corrections (for $\xi = 0$) in the Standard Model potential are indeed small. Figure 7 verifies for $\xi = 0$ that the gradient contribution to R is significant in the interior of the bubble; R peaks at the *positive* value $R/M_{\rm P}^2 = 2.213 \times 10^{-8}$ when $\phi(\chi_{\rm peak}) \approx 10^{17}$ GeV, at which point $V < 0$. This suggests a physical explanation for why the thin-wall approximation overestimates the suppression of vacuum decay: in the interior of the bubble the thin-wall approximation assumes that the only contribution to $\dot{a}$ is from the true vacuum, i.e.,

$$\dot{a}^2 \approx 1 - \frac{a^2 V(\phi_{\rm tv})}{3M_p^2}. \tag{18}$$

This would correspond to $R < 0$ and so the $R > 0$ region of Fig. 7 demonstrates that the approximation has completely broken down. Physically speaking, the backreaction due to the energy density in the interior of the bubble suppresses the decay rate because it decreases the bubble's volume-to-surface-area ratio compared to flat space (see Ref. [13]); this means an energy-conserving bubble must be larger. As a result, nucleating such a bubble requires overcoming a greater gradient barrier and so the decay rate is suppressed. However, the backreaction of the bubble walls, which the thin-wall approximation neglects, counteracts this effect since for $R > 0$ the opposite is true; the volume-to-surface-area ratio of the bubble increases. The net result is that the interior backreaction wins, but with a much reduced suppression of the decay rate. This is in addition to the fact that thick-wall bubbles do not touch the true vacuum, which also reduces $|R|$.

B. Effect of nonminimal coupling

The situation for $\xi \neq 0$ is somewhat different. Most notable is the near cancellation of the backreaction when $\xi = 1/6$, for which the bounce closely resembles the flat-space solution (see Fig. 3). Figure 4 demonstrates that $\xi = 1/6$ is near the minimal value for the decay exponent; the decay rate is virtually identical to flat space. The reason for this is that $\xi = 1/6$ restores a near conformal symmetry to the bounce equations. Consider the situation where

$V(\phi) = \lambda\phi^4/4$, for constant $\lambda < 0$. Such a potential has a conformal symmetry and for $\xi = 1/6$ the equations are, therefore, exactly conformal. The Ricci scalar satisfies Eq. (11) and for $\xi = 1/6$ the $\dot{\phi}^2(1-6\xi)$ term vanishes. Additionally, the second and third terms cancel:

$$4V(\phi) - 6\xi\phi V'(\phi) = \lambda\phi^4 - \frac{6}{6}\phi\cdot\lambda\phi^3 = 0. \quad (19)$$

Thus $R = 0$ holds everywhere for this exactly conformal situation and the backreaction cancels exactly. It is a simple matter to show that the $\frac{3\dot{a}}{a}$ term in Eq. (8) reduces to the flat-space case as well:

$$\begin{aligned} R &= \frac{6(1-\dot{a}^2)}{a^2} - \frac{6\ddot{a}}{a} = 0 \Rightarrow 1 - \dot{a}^2 - \ddot{a}a \\ &= 1 - \frac{\mathrm{d}}{\mathrm{d}\chi}(\dot{a}a) = 0 \\ &\Rightarrow \dot{a}a = \chi + C \Rightarrow \\ \frac{1}{2}\frac{\mathrm{d}}{\mathrm{d}\chi}(a^2) &= \chi + C \Rightarrow a(\chi) = \sqrt{\chi^2 + 2C\chi + D}, \end{aligned}$$

where C and D are integration constants. To match the boundary conditions $a(0) = 0, \dot{a}(0) = 1$, it is clear that $a(\chi) = \chi$. Thus, the bounce equations reduce to

$$\ddot{\phi} + \frac{3}{\chi}\dot{\phi} + |\lambda|\phi^3 = 0. \quad (20)$$

This is exactly the flat-space bounce equation. Therefore, in the case of $\xi = 1/6$ an analytic expression for the solution can be found in the form of the flat-space Lee-Weinberg bounce [37]:

$$\phi(\chi) = \sqrt{\frac{2}{|\lambda|}}\frac{2\bar{R}}{(\chi^2 + \bar{R}^2)}, \quad (21)$$

where $\bar{R}$ is an arbitrary scale arising due to the exact conformal symmetry. In the case of the Standard Model, the running of λ breaks this conformal symmetry. However, the contribution to the Ricci scalar still nearly cancels:

$$4V(\phi) - 6\xi\phi V'(\phi) = -\lambda'(\phi)\frac{\phi^5}{4} = -\frac{\mathrm{d}\lambda}{\mathrm{d}\ln(\phi^2/M^2)}\frac{\phi^4}{2}; \quad (22)$$

it is straightforward to verify numerically that $\mathrm{d}\lambda/\mathrm{d}\ln(\phi^2/M^2)$ is small. For example, at $M_h = 125.15\,\mathrm{GeV}$, $M_t = 173.34\,\mathrm{GeV}$, $|\beta_\lambda| = |\mathrm{d}\lambda/\mathrm{d}\ln(\phi^2/M^2)| < 1.1\times10^{-2}$ over the whole range of μ up to the Planck scale. Also, since the scale of the peak of the bounce is dominated by the scale at which β_λ vanishes, β_λ is by definition tiny in the vicinity of the peak; this is precisely the region when ϕ is close to the Planck mass and gravitational effects would matter most. Thus, the bounce for $\xi = 1/6$ in the Standard Model should have $R \approx 0$ and thus be approximately the same as the flat-space case. This is precisely what our numerical results show; the bounce is almost identical to the flat-space bounce except for a small difference near the peak (see inset Fig. 3), where the slightly broken conformal symmetry leads to small backreaction effects.

To compare the level of backreaction in each case, we plot the Ricci-scalar for the $\xi = 0, \xi = 1/6$, and $\xi = 1/3$ cases in Fig. 7. This demonstrates a significant suppression of the backreaction, quantified by R. For $\xi = 1/6$, the backreaction is not entirely suppressed, due to the running of λ breaking the conformal symmetry. Away from $\xi = 1/6$, Fig. 4 shows that B increases in both directions; this indicates that the effect of ξ is always to suppress vacuum decay, if the false vacuum is flat. As mentioned in the results section, this effect persists to larger values of $|\xi|$. The degree of suppression is evident in Fig. 6, which shows the boundary between stability and instability is pushed back as $|\xi|$ increases (middle region). The effect of pure backreaction ($\xi = 0$) is also to push back the boundary, although the effect is small.

It is worth noting that since the 3-sigma bounds on the top quark and Higgs masses do not place the Standard Model near the instability boundary, the effect of nonminimal coupling does not qualitatively change the decay behavior of the Higgs field, other than increasing its lifetime. In our analysis, the boundary between stability and metastability does not change, because whether or not the electroweak vacuum is false is determined in the Einstein frame by Eq. (4). With $\xi = 0$ the electroweak vacuum is stable if $V(\phi)$ is nowhere negative, and metastable (or unstable) otherwise. Equation (4) does not affect the sign of V, nor where it changes sign (the instability scale, ϕ_{inst}), and so the only effect of ξ is to change (in this case decrease) the actual decay rate, if the vacuum is not stable. A completely stable vacuum remains stable when nonminimal coupling is included. Note that this is not the case in a nonflat background, i.e., $V(\phi_{\mathrm{fv}}) \neq 0$, since there the criterion for stability is that $V(\phi) \geq V(\phi_{\mathrm{fv}})$ everywhere, rather than $V(\phi) \geq 0$. So, for example, if $\phi_{\mathrm{fv}} = 0, \xi > 0$ and $V(0) > 0$ is sufficiently large, then $\tilde{V}(0) = V(0)$ and the difference

$$\tilde{V}(\phi) - \tilde{V}(0) = \frac{\Delta V(\phi) + [1 - \left(1 - \frac{\xi\phi^2}{M_{\mathrm{P}}^2}\right)^2]V(0)}{\left(1 - \frac{\xi\phi^2}{M_{\mathrm{P}}^2}\right)^2}, \quad (23)$$

where $\Delta V(\phi) = V(\phi) - V(\phi_{\mathrm{fv}})$, can always be made positive for any negative $\Delta V(\phi)$, if $V(0)$ is sufficiently large. In the Jordan frame, this manifests as an extra mass term $\frac{1}{2}\frac{4V(0)}{M_{\mathrm{P}}^2}\phi^2$ in the potential. For $V(\phi_{\mathrm{fv}}) = 0$, however, this effect is not present and $\xi > 0$ will not render the false

vacuum absolutely stable unless $\xi > M_P^2/\phi_{\rm inst}^2$, i.e., the instability scale $\phi_{\rm inst}$ is above the threshold for which a singularity appears in the equations of motion. There is a caveat to the above, however; the stability/metastability boundary can in fact shift from the estimate based on the sign of the potential, since in the strong gravity limit it is possible for the gravitational effects of bounces to AdS true vacua to fully quench vacuum decay. This was investigated recently in Ref. [19], where it was found that the quenching effect present in the thin-wall approximation persisted for thick-wall bubbles, and when all gravitational effects were taken into account. We do not investigate this effect here, but it can in principle lead to shifts in the stability/metastability boundary.

C. Exact minimum under ξ variation

The form of Fig. 4 appears to suggest a minimum near $\xi = 1/6$. Assuming that $B(\xi)$ and $\phi_\xi(\chi)$ (the bounce solution with nonminimal coupling ξ) vary smoothly with ξ, we can construct an analytic expression for $B'(\xi)$. Recall that $B = S - S_{\rm fv}$ where $S_{\rm fv}$ is the false vacuum action. Assuming that the false vacuum lies at $\phi = 0$ for all ξ, then $S_{\rm fv}$ is independent of ξ because $R = 0$ for that solution (this would not be the case for a transition from a de Sitter false vacuum, however). Consequently, we can write

$$\frac{dB}{d\xi} = \left.\frac{\partial S_\xi[\phi_\xi, g_{\xi,\mu\nu}]}{\partial \xi}\right|_{\phi, g_{\mu\nu}} + \left.\frac{\delta S_\xi[\phi_\xi, g_{\xi,\mu\nu}]}{\delta \phi}\right|_{\xi, g_{\mu\nu}} \frac{\partial \phi_\xi}{\partial \xi} + \left.\frac{\delta S_\xi[\phi_\xi, g_{\xi,\mu\nu}]}{\delta g_\xi^{\mu\nu}}\right|_{\xi,\phi} \frac{\partial g_\xi^{\mu\nu}}{\partial \xi} \tag{24}$$

where ϕ_ξ and $g_{\xi,\mu\nu}$ are the scalar field and metric bounce solutions respectively, when the action is S_ξ defined by

$$S_\xi[\phi, g_{\mu\nu}] \equiv \int d^4x \sqrt{g}\left[\frac{1}{2}\nabla_\mu\phi\nabla^\mu\phi + V(\phi) + \frac{1}{2}\xi\phi^2 R - \frac{M_P^2}{2}R\right]. \tag{25}$$

Defining a new functional

$$\left.\frac{\partial S_\xi}{\partial \xi}\right|_{\phi, g_{\mu\nu}} = \Delta S[\phi, g_{\mu\nu}] \equiv \int d^4x \frac{1}{2}\phi^2 R, \tag{26}$$

and using the fact that the first functional derivatives of S_ξ at $\phi_\xi, g_{\xi,\mu\nu}$ vanish (as these are stationary points of S_ξ), we find

$$\frac{dB}{d\xi} = \pi^2 \int_0^\infty d\chi a_\xi^3(\chi)\phi_\xi^2(\chi)R_\xi(\chi). \tag{27}$$

All the quantities in the integrand can be evaluated from the bounce solution, once it is found. We confirmed that this prediction for the derivative of $B(\xi)$ agrees with numerical differentiation of the data in Fig. 4. Equation (27), however, yields useful analytic insight into the shape of Fig. 4. In particular, it reveals that $\xi = 1/6$ would be the exact minimum of the potential for a constant λ quartic potential, since Eq. (19) shows that the Ricci scalar vanishes everywhere for $\xi = 1/6$, and hence $B'(\xi) = 0$. In the Standard Model, the conformal symmetry of the large-scale Higgs potential is broken by the running of λ, which manifests in the nonvanishing of R (see Fig. 7). Consequently, the minimum shifts to a value slightly different from $\xi = 1/6$. The near vanishing of R for $\xi = 1/6$, however, explains the observation that Fig. 4 has a minimum very close to $\xi = 1/6$. The exact minimum can be found by a root-finding algorithm using Eq. (27). For example, if $M_h = 125.15$ GeV and $M_t = 173.34$ GeV the minimum lies at $\xi_{\rm min} = 0.16676$, a shift of $\xi_{\rm min} - 1/6 = 9.3354 \times 10^{-5}$.

D. Comparison to previous results

The authors of Ref. [14] previously computed an analytic correction to the bounce action via a perturbation expansion in the gravitational coupling, $\kappa = \frac{1}{M_P^2}$, or more precisely, the dimensionless quantity $1/(\bar{R}^2 M_P^2)$ where $\bar{R}$ is the bounce length scale [see Eq. (21)]:

$$\phi(\chi) = \phi_0(\chi) + \kappa\phi_1(\chi) + O(\kappa^2), \tag{28}$$

$$a(\chi) = a_0(\chi) + \kappa a_1(\chi) + O(\kappa^2) \tag{29}$$

where $a_0(\chi) = \chi$, and ϕ_0 is the flat-space bounce in the constant λ potential (which is more convenient to quantize around). Note for comparison that we define $M_P^2 = 1/8\pi G_N$, whereas the authors of Ref. [14] used $M_P^2 = 1/G_N$. However, it was recently pointed out [15] that when perturbed around the constant λ potential this perturbation expansion fails to satisfy the boundary conditions at first order in κ. This can be demonstrated by considering the equations for the first-order perturbations. Substituting the expansions into the bounce equations we obtain, comparing the first order in κ,

$$\ddot{\phi}_1 = -\frac{3}{\chi}\left(-\frac{a_1(\chi)}{\chi}\dot{\phi}_0 + \dot{\phi}_1 + \dot{a}_1\dot{\phi}_0\right) + V''(\phi_0)\phi_1, \tag{30}$$

$$\dot{a}_1 = \frac{\chi^2}{3}\frac{8\bar{R}^2}{|\lambda|}\frac{1}{(\chi^2+\bar{R}^2)^3},$$
$$\phi_0(\chi) = \sqrt{\frac{2}{|\lambda|}}\frac{2\bar{R}}{\bar{R}^2+\chi^2}, \quad \dot{\phi}_0 = -\sqrt{\frac{2}{|\lambda|}}\frac{4\bar{R}\chi}{(\bar{R}^2+\chi^2)^2}. \tag{31}$$

The equation for a_1 can be integrated immediately. Setting $x = \chi/\bar{R}$ and $y = \bar{R}^3|\lambda|^{3/2}\phi_1$ we find the equation for the first-order perturbation of the field is

$$y''(x)+\frac{3}{x}y'(x)+\frac{24}{(1+x^2)^2}y+\tilde{f}(x)=0,$$
$$\tilde{f}(x)\equiv 4\sqrt{2}\left(\frac{(x^2-1)}{(1+x^2)^4}+\frac{\arctan(x)}{x(1+x^2)^2}-\frac{8x^2}{(1+x^2)^5}\right). \quad (32)$$

The general solution to this equation is

$$\begin{aligned}y(x)=&\frac{C_1(x^2-1)}{(1+x^2)^2}\\&+\frac{C_2[1-17x^2-x^2(1-x^2)(x^2+12\ln x)]}{2x^2(1+x^2)^2}\\&+\frac{4\sqrt{2}}{45x^2(1+x^2)^3}\left[1+x^2(7-9x^2)\right.\\&\left.-15x^3(1+x^2)\arctan(x)+6x^2(1-x^4)\ln\left(\frac{1+x^2}{x^2}\right)\right].\end{aligned} \quad (33)$$

In the limit as $x\to\infty$ one finds $y(x)\to C_2/2$. When $x\to 0$ however, we obtain the asymptotic form

$$\begin{aligned}y(x)\to&\left(\frac{C_2}{2}+\frac{4\sqrt{2}}{45}\right)\left(\frac{1}{x^2}-12\ln x\right)\\&+\left(-C_1-\frac{19}{2}C_2+\frac{16\sqrt{2}}{45}\right)+O(x^2\ln x).\end{aligned} \quad (34)$$

Note that ϕ_0 satisfies $\dot{\phi}_0(0)=0, \phi_0(\chi\to\infty)\to 0$, and $\phi(\chi)$ is required to satisfy the same boundary conditions: this implies that $\phi_1(\chi)$ [and therefore $y(x)$, which is related to ϕ_1 by a constant factor] must satisfy the same conditions. Thus $y'(0)=0$ and $y(x\to\infty)\to 0$ are required. It is clear from the two limits of Eq. (33) that these boundary conditions cannot be simultaneously satisfied. If $y(x)$ is regular at $x=0$ then it tends to $-4\sqrt{2}/45$ as $x\to\infty$ and if it tends to zero (the false vacuum) at $x\to\infty$ then it will fail to be regular at $x=0$. This indicates that the perturbation expansion, Eq. (28), always breaks down for some values of χ and hence the solution seemingly cannot be trusted. Note that after this paper was submitted, a more detailed explanation of the perturbative procedure was published which we feel alleviates this concern; see Ref. [38]. The above argument demonstrates that the gravitationally corrected perturbative bounce solution would not exist in a ϕ^4 potential due to the breakdown of the perturbation theory at late χ. In Ref. [38], however, it was pointed out that the ϕ_1 correction should properly be determined in a quantum-corrected potential, rather than the $\lambda\phi^4$ potential, for which the behavior at large χ is different.

To compare with the perturbative prediction, assuming minimal coupling, we use the perturbative formula for first-order gravitational corrections to a generic flat-space bounce, $\Delta S_{\rm grav}=S_{\rm grav}-S_{\rm flat}$ (see Ref. [14]):

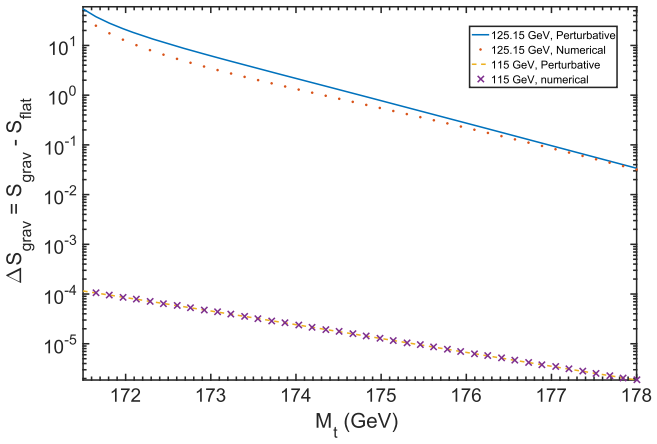

FIG. 8. Comparison of the perturbative results, Eq. (35), to our numerical calculations in the full Standard Model potential, for $M_h=125.15$ GeV and $M_h=115$ GeV.

$$\begin{aligned}\Delta S_{\rm grav}=&\frac{6\pi^2}{M_{\rm P}^2}\int_0^\infty d\chi\left[\chi^2\left(\frac{\dot{\phi}_0^2}{2}+V(\phi_0)\right)a_1\right.\\&\left.+(\chi\dot{a}_1^2+2a_1\dot{a}_1+2\chi a_1\ddot{a}_1)\right]\\=&\frac{6\pi^2}{M_{\rm P}^2}\int_0^\infty d\chi\dot{a}_1^2\chi\\=&\frac{\pi^2}{6M_{\rm P}^2}\int_0^\infty\chi^5\left[\frac{\dot{\phi}_0(\chi)^2}{2}-V(\phi_0(\chi))\right]^2 d\chi,\end{aligned} \quad (35)$$

where (see Ref. [14])

$$\dot{a}_1=\frac{\chi^2}{6}\left(\frac{\dot{\phi}_0^2}{2}-V(\phi_0)\right), \quad (36)$$

$$\ddot{a}_1=-\frac{\chi}{3}(\dot{\phi}_0^2+V(\phi_0)). \quad (37)$$

To compare the size of the gravitational corrections, we plot (see Fig. 8) $\Delta S_{\rm grav}=S_{\rm grav}-S_{\rm flat}$, using the numerically determined (flat-space) ϕ_0 in Eq. (35) for different M_t, M_h, and compare with the action predicted by numerically solving for the bounce including gravity. Our results broadly agree with this perturbative calculation: for $M_h=115$ GeV the agreement is excellent, as for this value of the Higgs mass the gravitational corrections are small and well approximated by the perturbative results. For $M_h=125.15$ GeV, closer to the best current measurements, the numerical results predict a slightly smaller decay rate, as higher-order terms in the gravitational perturbation series start to become important.

VI. CONCLUSION

We have computed the full gravitational effects on bounces in the Standard Model. For the region of interest,

the effect on the stability bounds of pure ($\xi = 0$) backreaction is almost negligible. Our results are broadly in line with the perturbative results. Furthermore, we have computed, for what we believe is the first time, the effect on the decay rate of including a nonminimal coupling term in the action. (After this paper was submitted, a perturbative calculation of the effect of nonminimal coupling was presented in Ref. [38], using a perturbative analysis; this gave broadly similar results.) We found that gravitational effects suppress vacuum decay universally for all values of the nonminimal coupling and push back the boundary between instability and stability. The effect, however, would not stabilize the potential completely because it does not change the location of the boundary between the stable/metastable regions of (M_h, M_t) phase space. Our calculations singled out the conformal value of $\xi = 1/6$ as being particularly special. For this value of the nonminimal coupling the effect of backreaction was found to nearly cancel, with the cancellation failing to be exact due to the running of the Higgs self-coupling, $\lambda(\mu)$, which breaks the conformal symmetry. $\xi = 1/6$ is also a near minimum of the decay exponent as a function of ξ. We showed that in an exactly conformal potential with $\xi = 1/6$ (a) the backreaction completely cancels, (b) the bounce solution is identical to the flat-space bounce, and (c) the decay exponent is minimal under ξ variations. Each of these properties is found to nearly hold in the full Standard Model potential, as it is "nearly" conformal at large field values.

Our results show that minimal-coupling gravitational effects in computing Standard Model vacuum decay rates are small, and provide a first analysis of the impact of nonminimal coupling. There is still much to be understood about the effect of gravity and nonminimal coupling on vacuum decay, however. For example, our results do not take into account the running of ξ, which should be present in a complete description of its effect on vacuum decay. We also do not take into account the effect of graviton loops on the running of the Standard Model couplings. A proper analysis of these issues will require a study of the quantum corrections to the gravitational bounce in the form of the functional determinant prefactor, A, in Eq. (1). Additionally, as mentioned in the discussion, there may be a shift in the stability/metastability boundary associated with the quenching effect of AdS true vacua [19]. The nature of this effect when nonminimal coupling is included is a natural direction for further investigation. Finally, the role of nonminimal coupling in nonflat backgrounds, for example during inflation, is also an important avenue for further study because it is possible for nonminimal coupling to stabilize the Standard Model potential if $V(\phi_{\rm fv}) > 0$ [10]. Such an analysis could therefore provide useful insight into the implications of vacuum metastability for early Universe physics.

ACKNOWLEDGMENTS

We thank Erick Weinberg and Tommi Markkanen for useful discussions, as well as the authors of Refs. [14,38] for useful comments regarding the interpretation of their perturbative results. A. R. was supported by STFC (Science and Technology Facilities Council) grant ST/L00044X/1, and S. S. by the Imperial College PhD Scholarship.

APPENDIX: EINSTEIN FRAME ANALYSIS

The action and field equations in the Einstein frame are obtained by a conformal transformation

$$\tilde{g}_{\mu\nu} = \Omega^2 g_{\mu\nu}, \tag{A1}$$

$$\Omega^2 \equiv \left(1 - \frac{\xi\phi^2}{M_{\rm P}^2}\right), \tag{A2}$$

and the field transformation

$$\mathrm{d}\tilde{\phi} = \frac{\sqrt{1 - \xi(1-6\xi)\frac{\phi^2}{M_{\rm P}^2}}}{\left(1 - \frac{\xi\phi^2}{M_{\rm P}^2}\right)}\mathrm{d}\phi \tag{A3}$$

$$\Rightarrow \tilde{\phi}(\phi) = M_{\rm P}\sqrt{6}\,\mathrm{arctanh}\left(\frac{\xi\sqrt{6}\phi}{M_{\rm P}\sqrt{1 - \frac{\xi(1-6\xi)\phi^2}{M_{\rm P}^2}}}\right) + M_{\rm P}\sqrt{\frac{1-6\xi}{\xi}}\,\mathrm{arcsin}\left(\sqrt{\xi(1-6\xi)}\frac{\phi}{M_{\rm P}}\right). \tag{A4}$$

Under these transformations, Eq. (2) becomes [39,40]

$$S = \int \mathrm{d}^4x\sqrt{|\tilde{g}|}\left[\frac{1}{2}\tilde{g}^{\mu\nu}\nabla_\mu\tilde{\phi}\nabla_\nu\tilde{\phi} + \frac{V(\phi(\tilde{\phi}))}{\left(1 - \frac{\xi\phi(\tilde{\phi})^2}{M_{\rm P}^2}\right)^2} - \frac{M_{\rm P}^2}{2}\tilde{R}\right]. \tag{A5}$$

Choosing an analogous coordinate system to Eq. (7) for the conformally transformed metric gives the bounce equation:

$$\frac{\mathrm{d}^2\tilde{\phi}}{\mathrm{d}\tilde{\chi}^2} + 3\frac{\frac{\mathrm{d}\tilde{a}}{\mathrm{d}\tilde{\chi}}}{\tilde{a}}\frac{\mathrm{d}\tilde{\phi}}{\mathrm{d}\tilde{\chi}} - \frac{\mathrm{d}}{\mathrm{d}\tilde{\phi}}\left[\frac{V(\phi(\tilde{\phi}))}{\left(1 - \frac{\xi\phi(\tilde{\phi})^2}{M_{\rm P}^2}\right)^2}\right] = 0, \tag{A6}$$

where

$$\mathrm{d}\tilde{\chi}^2 = (1 - \xi\phi^2/M_{\rm P}^2)\mathrm{d}\chi^2, \tag{A7}$$

$$\tilde{a}^2 = (1 - \xi\phi^2/M_{\rm P}^2)a^2, \tag{A8}$$

$$d\tilde{\phi} = \frac{\sqrt{1-\xi(1-6\xi)\phi^2/M_P^2}}{(1-\xi\phi^2/M_P^2)}d\phi. \tag{A9}$$

As mentioned previously, Eq. (A9) can be integrated to obtain $\tilde{\phi}(\phi)$, but the result cannot easily be inverted, analytically, for arbitrary ξ. This makes Eq. (A6) of limited use for numerics, but it can still reveal qualitative features of the solution which are somewhat more opaque in Eq. (8).

Making the variable changes (A7)–(A9) transforms Eq. (8) into Eq. (A6). Furthermore, the locations of the true and false vacua are determined by the Einstein frame potential, rather than $V(\phi)$. This is true in both the Einstein and Jordan frames. To see this, consider $\phi''(0)$ in both frames:

$$\phi''_{\rm Jordan}(0) = \frac{V'(\phi_0)(1-\frac{\xi\phi_0^2}{M_P^2}) + \frac{4\xi\phi_0 V(\phi_0)}{M_P^2}}{4\left(1-\frac{\xi(1-6\xi)\phi_0^2}{M_{P^2}}\right)}, \tag{A10}$$

$$\begin{aligned}\tilde{\phi}''_{\rm Einstein}(0) &= \frac{\tilde{V}'(\tilde{\phi}_0)}{4} \\ &= \frac{V'(\phi_0(\tilde{\phi}_0))\left(1-\frac{\xi\phi_0(\tilde{\phi}_0)^2}{M_P^2}\right) + \frac{4V(\phi_0(\tilde{\phi}_0))\xi\phi_0(\tilde{\phi}_0))}{M_P^2}}{4\left(1-\frac{\xi\phi_0(\tilde{\phi}_0)^2}{M_P^2}\right)^3}.\end{aligned} \tag{A11}$$

While these are different functions of ϕ_0—as we would expect—notice that they both have zeros at the same values of ϕ_0. For Coleman–de Luccia bounces, and in the Einstein frame, these critical points are merely the locations of the true vacuum, false vacuum, and the top of the barrier of the potential, respectively, as they are determined by the locations of the zeros of $\tilde{V}'(\tilde{\phi})$. Importantly, however, this is *not* the case if $\xi \neq 0$ in the Jordan frame: a field sitting initially at a point where $V'(\phi) = 0$ will generically start moving for $\xi \neq 0$ rather than staying constant. It is in fact the Einstein-frame potential, Eq. (4), which determines the location of these critical points. In the case of a fixed de Sitter background, this is equivalent to adding a $\frac{1}{2}\xi R\phi^2$ mass term.

[1] G. Aad *et al.*, Phys. Lett. B **716**, 1 (2012).
[2] S. Chatrchyan *et al.*, Phys. Lett. B **716**, 30 (2012).
[3] M. Sher, Phys. Rep. **179**, 273 (1989).
[4] S. Alekhin, A. Djouadi, and S. Moch, Phys. Lett. B **716**, 214 (2012).
[5] G. Degrassi, S. Di Vita, J. Elias-Miró, J. R. Espinosa, G. F. Giudice, G. Isidori, and A. Strumia, J. High Energy Phys. 08 (2012) 098.
[6] D. Buttazzo, G. Degrassi, P. P. Giardino, G. F. Giudice, F. Sala, A. Salvio, and A. Strumia, J. High Energy Phys. 12 (2013) 089.
[7] A. Kobakhidze and A. Spencer-Smith, Phys. Lett. B **722**, 130 (2013).
[8] V. Branchina, E. Messina, and A. Platania, J. High Energy Phys. 09 (2014) 182.
[9] M. Fairbairn and R. Hogan, Phys. Rev. Lett. **112**, 201801 (2014).
[10] M. Herranen, T. Markkanen, S. Nurmi, and A. Rajantie, Phys. Rev. Lett. **113**, 211102 (2014).
[11] M. Herranen, T. Markkanen, S. Nurmi, and A. Rajantie, Phys. Rev. Lett. **115**, 241301 (2015).
[12] G. Isidori, G. Ridolfi, and A. Strumia, Nucl. Phys. **B609**, 387 (2001).
[13] S. Coleman and F. De Luccia, Phys. Rev. D **21**, 3305 (1980).
[14] G. Isidori, V. S. Rychkov, A. Strumia, and N. Tetradis, Phys. Rev. D **77**, 025034 (2008).
[15] V. Branchina, E. Messina, and D. Zappala, Europhys. Lett. **116**, 21001 (2016).
[16] R. Gregory, I. G. Moss, and B. Withers, J. High Energy Phys. 03 (2014) 081.
[17] P. Burda, R. Gregory, and I. G. Moss, J. High Energy Phys. 08 (2015) 114.
[18] P. Burda, R. Gregory, and I. Moss, J. High Energy Phys. 06 (2016) 025.
[19] A. Masoumi, S. Paban, and E. J. Weinberg, Phys. Rev. D **94**, 025023 (2016).
[20] D. Z. Freedman, I. J. Muzinich, and E. J. Weinberg, Ann. Phys. (N.Y.) **87**, 95 (1974).
[21] A. V. Bednyakov, A. F. Pikelner, and V. N. Velizhanin, J. High Energy Phys. 01 (2013) 017.
[22] M. F. Zoller, in 17th International Moscow School of Physics (42nd ITEP Winter School) Moscow, Russian Federation, February 11–18, 2014 (to be published), arXiv:1411.2843.
[23] S. Coleman, Phys. Rev. D **16**, 1248 (1977).
[24] G. W. Gibbons and S. W. Hawking, Phys. Rev. D **15**, 2752 (1977).
[25] S. Coleman, V. Glaser, and A. Martin, Commun. Math. Phys. **58**, 211 (1978).
[26] J. Garriga and A. Megevand, Int. J. Theor. Phys. **43**, 883 (2004).
[27] A. Masoumi and E. J. Weinberg, Phys. Rev. D **86**, 104029 (2012).
[28] A. R. Brown and E. J. Weinberg, Phys. Rev. D **76**, 064003 (2007).
[29] L. G. Jensen and P. J. Steinhardt, Nucl. Phys. **B237**, 176 (1984).
[30] K. Ahnert and M. Mulansky, AIP Conf. Proc. **1389** (2011).
[31] L. Fousse, G. Hanrot, V. Lefèvre, P. Pélissier, and P. Zimmermann, ACM Trans. Math. Softw. **33**, 13 (2007).

[32] B. Gladman, MPFR, https://github.com/BrianGladman/mpfr.git.
[33] W. Press, *Numerical Recipes: The Art of Scientific Computing*, 3rd ed. (Cambridge University Press, Cambridge, England, 2007).
[34] Y. Perl, A. Itai, and H. Avni, Commun. ACM **21**, 550 (1978).
[35] V. Branchina, E. Messina, and M. Sher, Phys. Rev. D **91**, 013003 (2015).
[36] K. A. Olive *et al.* (Particle Data Group), Chin. Phys. C **38**, 090001 (2014).
[37] K. Lee and E. J. Weinberg, Nucl. Phys. **B267**, 181 (1986).
[38] A. Salvio, A. Strumia, N. Tetradis, and A. Urbano, J. High Energy Phys. 09 (2016) 054.
[39] S. Carroll, *Spacetime and Geometry: An Introduction to General Relativity* (Addison Wesley Reading, MA, 2004).
[40] V. Faraoni, E. Gunzig, and P. Nardone, Fundam. Cosm. Phys. **20**, 121 (1999).